

# A few months-old storm-generated turbidite deposited in the Capbreton Canyon (Bay of Biscay, SW France)

T. Mulder(✉) · O. Weber · P. Anschutz · F. J. Jorissen · J.-M. Jouanneau

---

T. Mulder · O. Weber · P. Anschutz · F.J. Jorissen · J.-M. Jouanneau  
Département de Géologie et Océanographie, UMR 5805 EPOC, Université Bordeaux I, Avenue des  
Facultés, 33405 Talence cedex, France

---

✉ E-mail: t.mulder@geocean.u-bordeaux.fr

---

**Received:** 22 January 2001 / **Revision accepted:** 20 July 2001 / **Published online:** ■

---

**Abstract.** A gravity core taken in the canyon of Capbreton shows a succession of sedimentary facies which can be interpreted as three superimposed Bouma sequences. The turbiditic sequences are covered by an oxidised layer which contains live benthic foraminiferal faunas indicating a reprisal of hemipelagic deposition. Activities of  $^{234}\text{Th}$  and  $^{210}\text{Pb}$  suggest that the most recent turbidite was deposited between early December 1999 and mid-January 2000. During this period, the most probable natural event able to trigger a turbidity current was the violent storm which affected the French Atlantic coast on 27 December 1999. The turbidity current could have been caused by a sediment failure due to an excess in pore pressure generated by the storm waves, an increase of the littoral drift, or the dissipation of the along-coast water bulge through the canyon. This sub-Recent turbidite shows that the canyon experiences modern gravity processes, despite the lack of a direct connection with a major sediment source.

## Introduction

Although turbidity currents and turbidites have been known for half a century (Kuenen 1951, 1952a, 1952b, 1953, 1959; Bouma 1962), much controversy still exists concerning the processes of deposition (Kneller and Branney 1995; Shanmugam 1997, 2000; Mulder and Alexander 2001), their origin (Mulder and Cochonat 1996) and their recognition. Except for deposits related to processes in which the main particle-support mechanism is not turbulence, and which should not be termed "turbidites" (Middleton and Hampton 1973; Mulder and Alexander 2001), it is now clear that, even for real turbidites (i.e. sequences deposited by a turbulent flow; Shanmugam 2000), the Bouma sequence is not an ubiquitous model. Several exceptions of the classical model exist, such as the Lowe sequence (Lowe 1982) for coarse-grained turbidites, and the sequence defined for fine-grained turbidites (Stow and Shanmugam 1980; Piper and Stow 1991; Piper and Deptuck 1997). However, the conceptual model of Bouma (1962) remains valid for turbulent flows generated from sediment failure.

Turbidity currents are recognised as a major particle transport process in marine environments. They are at the origin of deep-sea turbiditic systems such as ramps fed by multiple sources, and deep-sea fans in which sediment is supplied by a linear source (Reading and Richards 1994). In both kinds of system, particles are transported through a canyon. A submarine canyon is defined as a sea valley with a V-shaped profile, high steep walls with rock outcrops, a winding course and numerous tributaries entering from both sides (Shepard and Dill 1966). Canyons are dominated by erosional processes. Their formation includes retrogressive failures and erosion by particle-laden gravity currents (Shepard 1981; Pratson et al. 1994). Turbidity currents have been indirectly observed in canyons on seismic profiles (Hay 1987; Viana 1997). Turbidity current activity is also indirectly indicated by cable failures on the Algerian slope (Heezen and Ewing 1955), in the Gulf of Corinth (Heezen and Hollister 1971), in the New Britain Trench (Krause et al. 1970), in the Var (Genesseeux et al. 1980), off the Grand Banks and Laurentian channel (Heezen and Ewing 1952; Hughes Clarke et al. 1990, 1992), and in the Zaire canyon (e.g. Shepard and Dill 1966; Droz et al. 1996). Measurements of an along-bottom turbid flow associated with velocities ranging from a few decimetres to a few metres per second are reported by Inman (1970), and Shepard et al. (1977, 1979) in La Jolla Canyon, by Genesseeux et al. (1971) in the Var canyon, and by Wright et al. (1986) in the Huanghe delta (China). Various processes can initiate submarine turbidity currents. Slope failure can be due to oversteepening or to an excess pore-water pressure. This excess pore pressure can be generated by gas seepage (Milkov 2000), high sedimentation rates, earthquake shaking (e.g. Heezen and Ewing 1952), high tides (Bjerrum 1971; Wisenam et al. 1986), and swell or storm waves (Prior et al. 1989). Turbidity currents can also be generated by river floods (Mulder and Syvitski 1995; Mulder and Alexander 2001).

In this paper, we demonstrate that a sedimentary sequence cored at 647-m water depth in the canyon of Capbreton results from deposition by a turbidity current generated by the violent storm which affected the French Atlantic coast at the end of December 1999.

## Geological setting

The canyon of Capbreton runs approximately parallel to the north coast of Spain. It is a 300-km-long meandering submarine valley. The canyon head cuts deeply into the continental shelf and is located only 250 m away from the coastline. The south wall escarpment bordering the Spanish shelf reaches up to 3,000 m at 133 km from the coastline. (Shepard and Dill 1966; Cirac et al. 2001). The canyon is 32 km wide at the most. The average slope of the canyon axis is 2.9% for the first 110 km, and 1.6% over the total canyon length. The canyon is not directly connected to any river at present, although direct connection with the Adour River existed until 1,310 A.D. At present, the Adour river mouth is located 15 km south of the canyon head. The main directions of the three parts of the channel (Fig. 1) are under structural control, as they follow the directions ENE-WSW and SE-NW of major regional faults which developed during the opening of the Bay of Biscay and the Pyrenean thrust (Boillot et al. 1972, 1974).

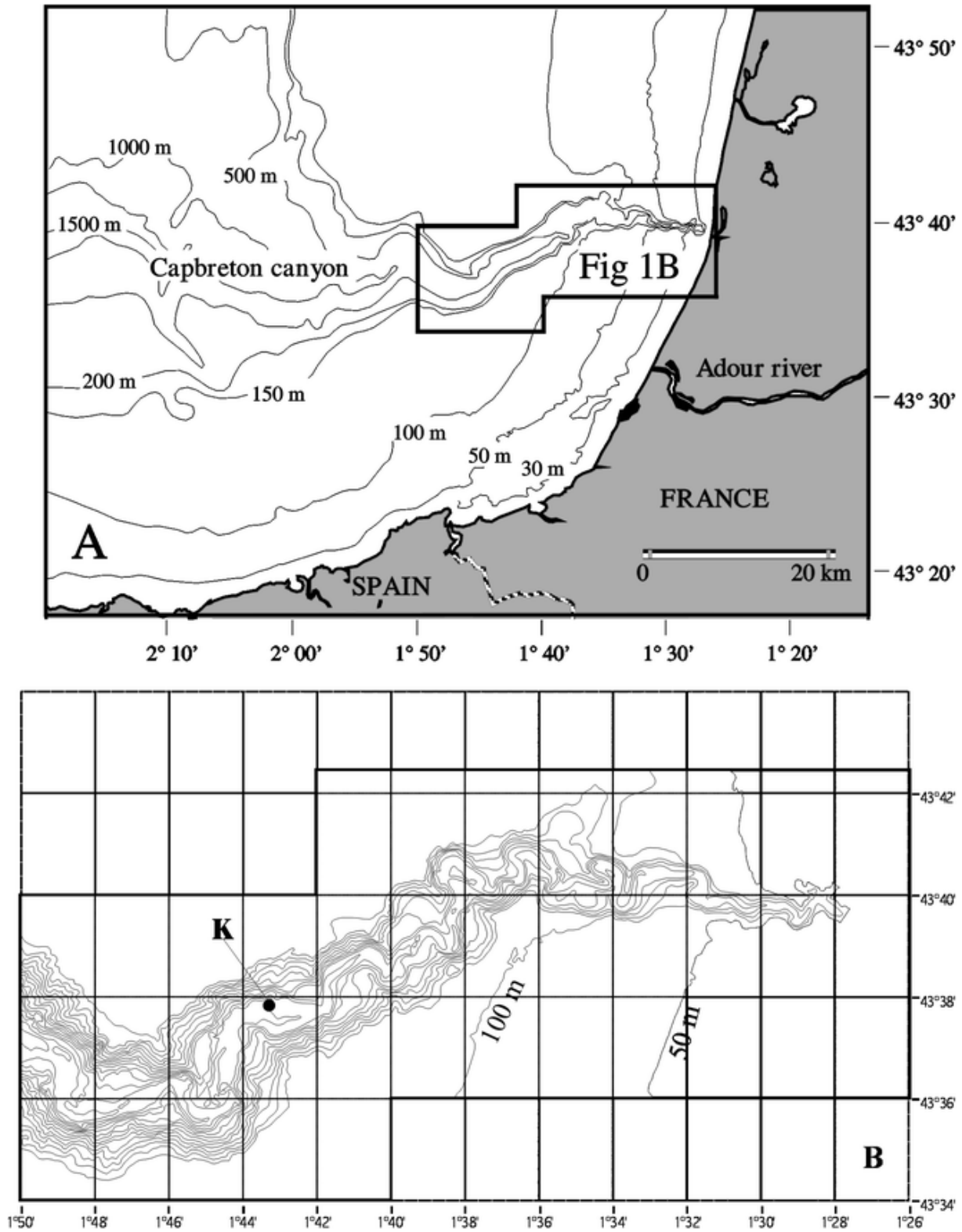


**Fig. 1.** **A** General map of the southern part of the Bay of Biscay showing the location of the Capbreton canyon. **B.** Detailed map of the study area showing the bathymetry of the Capbreton canyon and the location of core K. Contours in metres. Isobaths at 50-m intervals

---

## Materials and methods

A core was taken at station K ( $43^{\circ}37.833' \text{ N}$ ,  $1^{\circ}43.284' \text{ W}$ ) during the Oxybent 10 cruise (2 May 2000), using a classical Barnett interface gravity multicorer (Barnett et al. 1984). It is a 33-cm-long core located in the axis of the canyon at a water depth of 647 m (Fig. 1). A 1-cm-thick slab was sampled along the core length. This slab was X-radiographed using the Scopix system (Migeon et al. 1999), which consists of an X-ray imaging system combined with image analysis software. Subsampling for grain size and micropalaeontological analyses was performed using a particular procedure. Subsamples were positioned using a plastic Xerox copy of the X-ray image to accurately locate the laminae. After subsampling, the sampled slab was X-radiographed again to check the sample location and to verify that all the laminae had been sampled. Grain size was measured using a laser diffractometer Malvern Mastersizer. In addition, a large thin section was made to help interpretation.

The stratigraphic framework was provided by counting the activity of radiogenic isotopes:  $^{234}\text{Th}$  (half-life=24.1 days) and  $^{210}\text{Pb}$  (half-life=22.4 years). Counting for  $^{234}\text{Th}$  and  $^{210}\text{Pb}$  activities was performed over 20 h, using a high-resolution gamma spectrometer with a semiplanar detector (excess  $^{210}\text{Pb}=\text{total } ^{210}\text{Pb}-^{226}\text{Ra}$ ; excess  $^{234}\text{Th}=\text{total } ^{234}\text{Th}-^{226}\text{Ra}$ ).  $^{226}\text{Ra}$  is obtained from  $^{214}\text{Bi}$  and  $^{214}\text{Pb}$ . No activity can be detected after a period corresponding to six times the half-life at the maximum, i.e. 144 days for  $^{234}\text{Th}$ , and 122 years for  $^{210}\text{Pb}$ . The method is detailed in Jouanneau et al. (1988), and Gouleau et al. (2000).

Since  $^{234}\text{Th}$  has a very short half-life, we corrected the measured values (date of measurement is between 15 May 2000 and 2 June 2000) to take into account the time interval between core sampling (2 May 2000) and the measurements, using the classical exponential decay of radiogenic activity.

## Results

Figure 2 shows the sedimentological features of the entire core. X-ray analysis shows three units denoted S1, S2 and S3 from top to bottom (Fig. 2A and B). Sequences S1 and S2 are separated by an erosive contact. Sequences S2 and S3 are separated by a sharp contact. Ochre (10YR 6/5) oxidised layers containing benthic and planktonic foraminifers are located below each contact and at the top of the core. These oxidised layers are Mn- and Fe-enriched, which affects sediment colour and X-ray penetration.

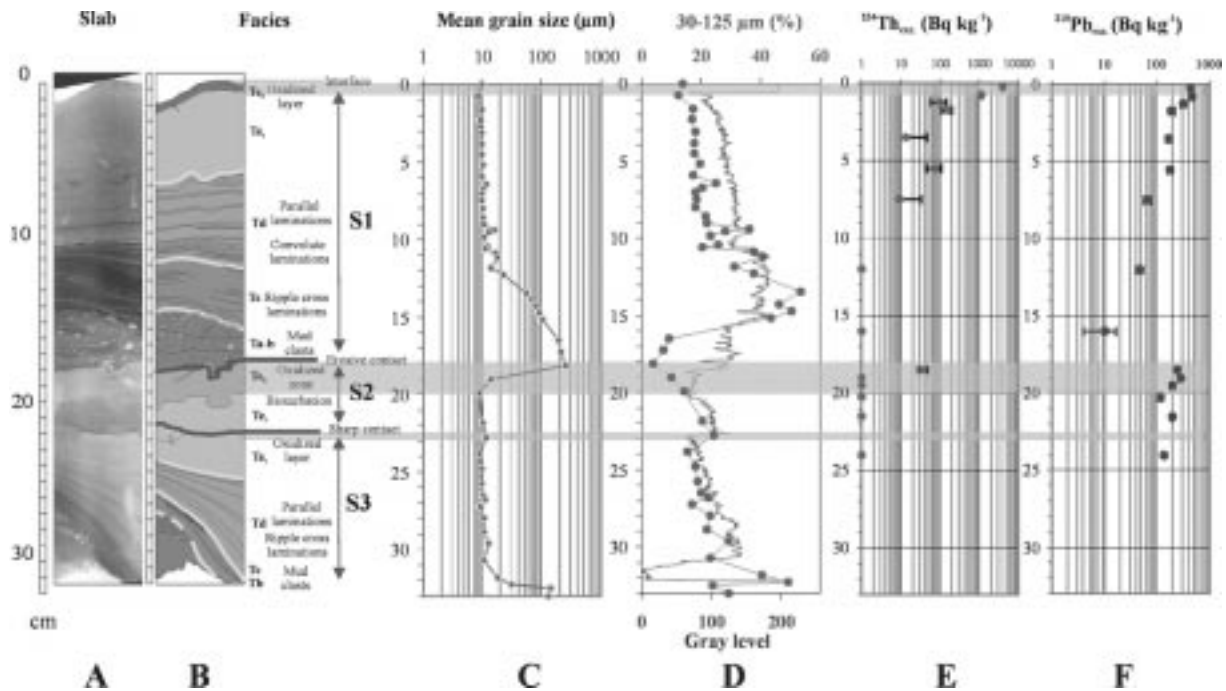


**Fig. 2A-F.** Sequence analysis of core K. **A** X-ray image. **B** Processed X-ray image (Scopix) and facies interpretation. **C** Grain-size distribution curve. **D** Grey level (plain line) and content of the 30-125  $\mu$  fraction (line with squares). **E** Curve of corrected  $^{234}\text{Th}_{\text{exc}}$  activity. **F** Curve of corrected  $^{210}\text{Pb}_{\text{exc}}$  activities

Sequence S3 is a fining-up sequence with its base missing, probably due to coring. Grain size grades up from fine sands to clayey silts. The base of the sequence shows a facies without structure but containing a few mud clasts. Above it, a cross-laminated facies can be observed, followed by a facies with parallel laminations located just below the oxidised layer separating S3 from S2.

Sequence S2 is 5 cm thick. It contains only a fine silty clay facies with slight bioturbation at its top, overlain by an oxidised layer.

Sequence S1 is the most complete sequence. It is a 18-cm-thick, fining-up sequence. The grey-level curve (on a 256-level scale; Fig. 2A) results from X-ray image analysis, and it depends on density (Bouma 1969) and porosity which, in turn, depend partly on grain size. In our case, it is sensitive to the medium-silt to fine-sand fractions. It is a valuable tool to accurately define facies limits. On Fig. 2D, the portion of the curve corresponding to sequence S1 shows three parts: (1) at the bottom, a part with a low grey level, indicating a small silt fraction due to a high sand content; (2) an intermediate part with a high grey level, indicating a high silt content; (3) at the top, a part with a low grey level, indicating a small silt fraction due to a high mud content. A facies consisting of clean sand with frequent mud clasts lies above the basal erosive contact. A cross-laminated facies, followed by a facies with convolute laminations and finally a facies with parallel laminations overlie it. It ends with a silty clay facies similar to the facies observed in S2, with slight bioturbation in the top last centimetre. A 5-mm-thick oxidised facies drapes the top of the core. The processed X-ray image of the core and selected grain-size distribution curves at different core levels are shown in Fig. 3.

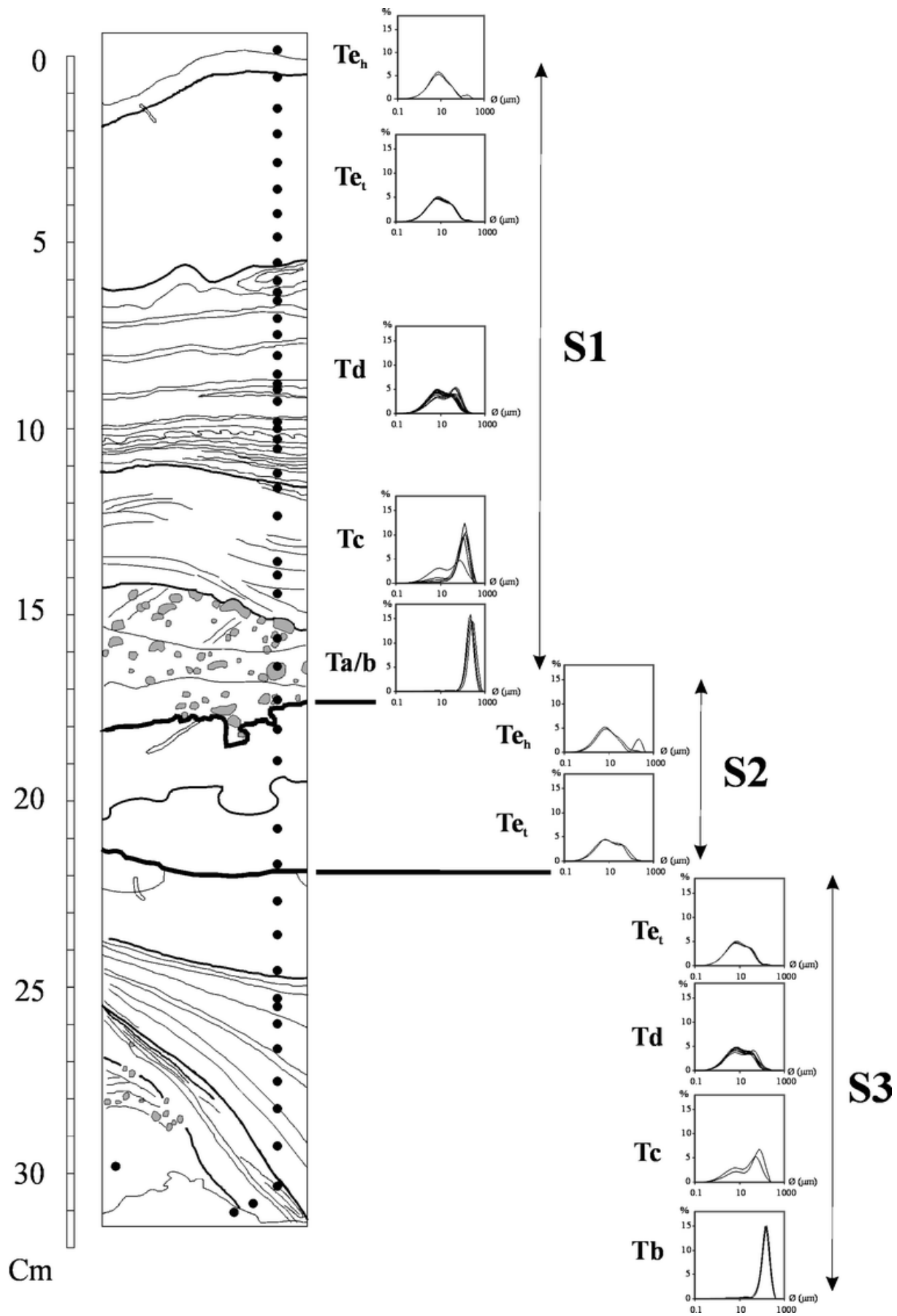


**Fig. 3.** Interpretation of the processed X-ray image showing the sampling locations and histograms of grain-size distributions in facies Ta to Te. Note progressively decreasing grain-size peak from facies Ta to Td

---

## Discussion

### Facies analysis

The facies succession and the progressive fining-up trend suggest that the three sequences observed in core K correspond to classical Bouma sequences (Bouma 1962; Shanmugam 1997). Fining-up trends indicate (Fig. 2C) deposition by suspension fall-out in the course of a progressively decreasing energy gradient at the core location. The data show the presence of structures which indicate that traction acts simultaneously to suspension fall-out. The clean sand facies without structures at the base of sequence S1 is interpreted as facies Ta of Bouma (1962). The facies with ripple-cross laminations and convolute laminations is interpreted as facies Tc in sequences S1 and S3. The facies with parallel horizontal laminations in sequences S1 and S3 is interpreted as facies Td. The nonlaminated facies at the top of the three sequences is interpreted as facies Te. Te is, in fact, the composite of a real turbiditic part ( $Te_t$ ), resulting from the deposition of the finest part of the turbiditic cloud and a subsequent hemipelagic part ( $Te_h$ ) resulting from reprisal of the background sedimentation. Facies Td-e corresponds to the part of the sequences with a low silt content caused by an important clay fraction. Facies Tb (which typically contains parallel horizontal laminations) seems to be absent or cannot be discriminated from Ta.

The distinction between the turbiditic and hemipelagic parts in Te can be made using the grain-size distribution curve for each facies (Fig. 3). Furthermore, the hemipelagic parts contain planktonic as well as autochthonous benthic foraminifers, whereas both are very scarce in the turbiditic part. In facies Ta to Td, the curves show peaks migrating progressively towards finer particles. The curves in facies Ta and Tb are unimodal and symmetrical. The curves in facies Tc, Td and  $Te_t$  are bimodal with two populations not clearly separated. The top part of Te, called  $Te_h$  and corresponding to the oxidised facies, shows either a symmetrical unimodal curve or a bimodal distribution with two clearly separated fractions with different amplitudes. Both fractions are interpreted as subfacies  $Te_h$  which is hemipelagic ooze.

Sequences S1, S2 and S3 correspond to the sedimentation from turbulent unsteady flows (surges). They are separated by hemipelagic, oxidised layers.

### Age of the sequences

The oxidised facies at the top of S1, between S1 and S2, or S2 and S3 all show high  $^{210}Pb_{exc.}$  activity, which suggests an age younger than 100 years for these three interfaces (Fig. 2F). The oxidised layer above S1 shows high values in  $^{234}Th_{exc.}$ , which is consistent with a strong input of  $^{234}Th_{exc.}$  after deposition of S1. The interface between S1 and S2 also shows high activity of  $^{234}Th_{exc.}$  (Fig. 2E), which suggests an age less than 144 days for this interface. In the oxidised interval between S1 and S2, the presence of benthic foraminifers which are still weakly stained by Rose Bengal suggests that the time interval following the deposition of S1 was not long enough for a complete decay of the foraminiferal protoplasm. The progressive decrease of radio-isotopic activity within the Ta-c facies of sequences is related only to the grain-size variation (cf. the downward decrease in clay content) and does not allow the calculation of accumulation rates. However, facies Td-e of S2 and S3 are mainly

composed of mud, and the accumulation rate and dating can be considered as reliable.

We consider that the flux of  $^{234}\text{Th}$  was identical at the time of deposition of the top of both S1 and S2. Calculations of the  $^{234}\text{Th}$  at the date of sampling suggest that sequence S2 was deposited before the period 18 November 1999 to 8 December 1999, and that the top of S1 ( $\text{Te}_t$ ) was deposited between 5 December 1999 and 14 January 2000. The dating of the oxidised layer at the bottom of S1 could be hampered due to erosion by the turbidity current which deposited S1. In this case the maximum ages for deposition of S1 would appear too old. According to Hyacinthe et al. (2001), the thickness of the oxidised layer does not exceed 1 cm in the Capbreton area. This suggests that the erosion below S1 is less than 5 mm. However, dating the upper part of the sequence shows high  $^{234}\text{Th}_{\text{exc}}$ , suggesting that the upper part was deposited before the end of January (Fig. 2). In addition, if the oxidised layer at the bottom of S1 had been intensely eroded, the grain-size distribution curves (Fig. 3) at the top and at the bottom of S1 would have different shapes. These curves are identical, suggesting only little erosion at the base of S1.

## Potential turbidite triggering mechanism

As the time range for the triggering period is very narrow, we investigated the potential cause for the triggering of the turbidity current which deposited sequence S1. No earthquake capable of generating a slope failure in the area was recorded during this period. There was no major flood at the mouth of the Adour River, which is the nearest river. The only natural phenomenon with the potential to trigger sediment movement during this period was the violent storm which hit the Bay of Biscay on 27 December 1999. Storms have previously been demonstrated as a triggering mechanism for turbidity currents in the Huanghe delta (Prior et al. 1989), off Hawaii (Normark and Piper 1991), and in the Titanic wreck area (Savoie et al. 1990). Storm-related hydrodynamic processes could also be involved in the initiation of small channels above the Albatross debris flow on the Scotian slope (Baltzer et al. 1994).

Storms can affect sediment stability in three different ways.

1. Swell and wave stress can generate excess pore pressure in sediments and reduce the shear resistance of the seafloor sediments down to failure. Such a process has been reported by Wright et al. (1986) in the Huanghe River. During the storm of 27 December 1999, waves with heights up to 12 m were recorded in the Bay of Biscay. Such high waves may have destabilised sediment on the shelf break adjacent to the core location, i.e. at a water depth of about 110 m or near the canyon head.
2. Shelf currents and coastal drift can be intensified during a storm. A large amount of particles can then be captured at the canyon head and progressively create a turbulent unsteady flow.
3. The eastward storm winds created a 1- to 2-m-high water bulge along the coast. The bulge could have dissipated, using the canyon as a natural sink. The violent downwelling currents may then have caused intensive particle erosion from the canyon head and down the channel, generating a particle-laden bottom layer which progressively transformed into a turbidity current. Such particle-rich downward and upward currents have already been observed during proxigean spring-tide conditions in La Jolla canyon (Shepard 1975). Fukushima et al. (1985) demonstrated that turbidity currents have been triggered in Scripps submarine canyon because of a modest agitation due to edge waves. Tide-related sediment advection has also been evidenced in the Huanghe delta (Wisnam et al. 1986). Then, the turbidity current can "ignite" (Parker 1982; Piper et al. 1992, 1999) - it self-accelerates by eroding particles from the bed.

In the present case, we cannot relate the present-day turbiditic activity to the processes at the head of the canyon. The amplitude of the storm waves provides a return period in the range of 10 years (Vassal 1980). This suggests that storm-related turbidity currents may be frequent in the Capbreton canyon.

## Conclusions

1. A sub-recent turbidite showing classical Bouma facies has been identified in the canyon of Capbreton, using both radiographic analysis for facies description and radio-isotope activity. This suggests that the canyon is currently active.
2. Dating suggests that the last turbidity current was triggered by the violent storm which occurred on 27 December 1999 in the Bay of Biscay.
3. The sequence deposited at 647-m water depth by this single event is 18 cm thick. This shows that turbidity currents can transport and deposit large volumes of sediment. The preservation of the previous sequence shows that vertical aggradation can be larger than erosion in some parts of the canyon. The frequency of the storm-related turbidity currents could lead locally to high accumulation rates.

*Acknowledgements.* This research was funded by the programme PROOF (INSU-CNRS). The authors thank the participants of the OXYBENT cruise and the crew of the RV Côtes de la Manche (INSU). Many thanks go to G. Chabaud for grain-size analysis, to J. Saint-Paul for slabbing and X-ray processing, and to B. Martin for thin sections. The authors also thank J.-C. Faugères, D.J.W Piper and P.P.E. Weaver for the review of this paper. This is contribution number 1411 of the UMR CNRS 5805 EPOC.

## References

- Baltzer A, Cochonat P, Piper DJW (1994) In situ geotechnical characterization of sediments on the Nova Scotian Slope, eastern Canadian continental margin. *Mar Geol* 120:291-308
- Barnett PRO, Watson J, Connelly D (1984) A multiple corer for taking virtually undisturbed samples from shelf, bathyal and abyssal sediments. *Oceanol Acta* 7:399-408
- Bjerrum L (1971) Subaqueous slope failures in Norwegian fjords. *Norge Geotech Bull* 88:1-8
- Boillot G, Dupeuble PA, Hennequin I (1972) Le plateau continental basque: stratigraphie, structure et relation avec le canyon de Capbreton. *C R Acad Sci Paris Sér D* 274:1147-1150
- Boillot G, Dupeuble PA, Hennequin-Marchand I, Lamboy M, Lepretre J-P, Musellec P (1974) Le rôle des décrochements "tardi-hercyniens" dans l'évolution structurale de la marge continentale et dans la localisation des grands canyons sous-marins à l'ouest et au nord de la péninsule ibérique. *Rev Géogr Phys Géol Dyn* (2) 16 (fasc 1):75-86
- Bouma AH (1962) *Sedimentology of some flysch deposits: a graphic approach to facies interpretation.* Elsevier, Amsterdam
- Bouma AH (1969) *Methods for the study of sedimentary structures.* Wiley, New York

Cirac P, Bourillet J-F, Griboulard R, Normand A, Mulder T, ITSAS Shipboard Scientific Party (2001) Le canyon de Capbreton: nouvelles approches morphostructurales et morphosédimentaires. Premiers résultats de la campagne Itsas. C R Acad Sci Paris 332:447-455

Droz L, Rigaut F, Cochonat P, Tofani R (1996) Morphology and recent evolution of the Zaire turbidite system (Gulf of Guinea). Geol Soc Am Bull 108:253-269

Fukushima Y, Parker G, Pantin HM (1985) Prediction of ignitive turbidity currents in Scripps submarine canyon. Mar Geol 67:55-81

Genesseeux M, Guibout P, Lacombe H (1971) Enregistrement de courants de turbidité dans la vallée sous-marine du Var (Alpes-Maritimes). C R Acad Sci Paris Sér D 273:2456-2459

Genesseeux M, Mauffret A, Pautot G (1980) Les glissements sous-marins de la pente continentale niçoise et la rupture de câbles en mer Ligure (Méditerranée occidentale). C R Acad Sci Paris Sér D 290:959-962

Gouleau D, Jouanneau J-M, Weber O, Sauriau PG (2000) Short term, long term sedimentation on Montportail-Brouage intertidal mudflat, western side of Marennes Oléron Bay (France). Cont Shelf Res 20:1513-1530

Hay AE (1987) Turbidity currents and submarine channel formation in Rupert Inlet, British Columbia. 2. The roles of continuous and surge-type flow. J Geophys Res 92:2883-2900

Heezen BC, Ewing M (1952) Turbidity currents and submarine slumps, and the 1929 Grand Banks earthquake. Am J Sci 250:849-873

Heezen BC, Ewing M (1955) Orléansville earthquake and turbidity currents. Am Assoc Petrol Geol Bull 39(12):2505-2514

Heezen BC, Hollister CD (1971) The face of the deep. Oxford University Press, New York

Hughes Clarke JE, Shor AN, Piper DJW, Mayer LA (1990) Large-scale current-induced erosion and deposition in the path of the 1929 Grand Banks turbidity current: Sedimentology 37:613-629

Hughes Clarke JE, O'Leary D, Piper DJW (1992) The relative importance of mass wasting and deep boundary current activity on the continental rise off western Nova Scotia. In: Poag CW, de Graciansky PC (eds) Geologic evolution of Atlantic continental rises. Van Nostrand Reinhold, New York, pp 266-281

Hyacinthe C, Anschutz P, Carbonel P, Jouanneau J-M, Jorissen FJ (2001) Early diagenetic processes in the muddy sediments of the Bay of Biscay. Mar Geol 177:111-128

Inman DL (1970) Strong currents in submarine canyons. Abstr Trans Am Geophys Union 51:319

Jouanneau J-M, Garcia C, Oliveira A, Rodrigues A, Dias JA, Weber O (1988) Dispersal and deposition of suspended sediment on the shelf off the Tagus and Sado estuaries, SW Portugal. Progr Oceanogr 42(1-4):233-257

Kneller BC, Branney MJ (1995) Sustained high-density turbidity currents and the deposition of thick massive beds. Sedimentology 42:607-616

- Krause DC, White WC, Piper DJW, Heezen BC (1970) Turbidity currents and cable breaks in the western Britain trench. *Geol Soc Am Bull* 8:2153-2160
- Kuenen PH (1951) Properties of turbidity currents of high density. In: Hough JL (ed) *Turbidity currents*. *Soc Econ Paleontol Mineral Spec Publ* 2:14-33
- Kuenen PH (1952a) Estimated size of the Grand Banks turbidity current. *Am J Sci* 250:849-873
- Kuenen PH (1952b) Paleogeographic significance of graded bedding and associated features. *Proc Konink Ned Akad Wetenschap* 20:1-47
- Kuenen PH (1953) Significant features of graded bedding. *Am Assoc Petrol Geol Bull* 37:1044-1066
- Kuenen PH (1959) Turbidity currents: a major factor in flysch deposition. *Eclogae Geol Helv* 51:1009-1021
- Lowe DR (1982) Sediment gravity flows. II. Depositional models with special reference to the deposits of high-density turbidity currents. *J Sediment Petrol* 52:279-297
- Middleton GV, Hampton MA (1973) Sediment gravity flows; mechanics of flow and deposition. In: Middleton GV, Bouma AH (eds) *Turbidites and deep water sedimentation*. *Soc Econ Paleontol Mineral Pacific Section Short Course Lecture Notes*, Anaheim, pp 1-38
- Migeon S, Weber O, Faugères J-C, Saint-Paul J (1999) SCOPIX: a new X-ray imaging system for core analysis. *Geo-Mar Lett* 18:251-255
- Milkov AV (2000) Worldwide distribution of submarine mud volcanoes and associated gas hydrates. *Mar Geol* 167:29-42
- Mulder T, Alexander J (2001) The physical character of subaqueous sedimentary density currents and their deposits. *Sedimentology* 48:269-299
- Mulder T, Cochonat P (1996) Classification of offshore mass movements. *J Sediment Res* 66:43-57
- Mulder T, Syvitski JPM (1995) Turbidity currents generated at river mouths during exceptional discharges to the world oceans. *J Geol* 103:285-299
- Normark WR, Piper DJW (1991) Initiation processes and flow evolution of turbidity currents: implications for the depositional record. In: Osborne RH (ed) *From shoreline to abyss*. *Contributions in marine geology in honor of Francis Parker Shepard*. *S EPM Spec Publ* 46:207-230
- Parker G (1982) Conditions for the ignition of catastrophically erosive turbidity currents. *Mar Geol* 46:307-327
- Piper DJW, Deptuck M (1997) Fine-grained turbidites of the Amazon fan: facies characterization and interpretation. In: Flood RD, Piper DJW, Klaus A, Peterson LC (eds) *Proceedings of the Ocean Drilling Program, Scientific Results* 155:79-108
- Piper DJW, Stow DAV (1991) Fine-grained turbidites. In: Einsele G, Ricken W, Seilacher A (eds) *Cycles and events in stratigraphy*. Springer, Berlin Heidelberg New York, pp 360-376

Piper DJW, Cochonat P, Ollier G, Le Dreezen E, Morrison M, Baltzer A (1992) Evolution progressive d'un glissement rotationnel en un courant de turbidité: cas du séisme de 1929 des Grands Bancs (Terre Neuve). *C R Acad Sci Paris Sér II* 314:1057-1064

Piper DJW, Cochonat P, Morrison ML (1999) The sequence of events around the epicentre of the 1929 Grand Bank earthquake: initiation of debris flows and turbidity current inferred from sidescan sonar. *Sedimentology* 46:79-97

Pratson LF, Ryan WBF, Mountain GS, Twichell DC (1994) Submarine canyon initiation by downslope-eroding sediment flows: evidence in late Cenozoic strata on the New Jersey continental slope. *Geol Soc Am Bull* 106:395-412

Prior DB, Suhayda JN, Lu NZ, Bornhold BD, Keller GH, Wiseman WJ, Wright LD, Yang Z-S (1989) Storm wave reactivation of a submarine landslide. *Nature* 341:47-50

Reading HG, Richards M (1994) Turbidite systems in deep-water basin margins classified by grain size and feeder system. *Am Assoc Petrol Geol Bull* 78:792-822

Savoie B, Cochonat P, Piper DJW (1990) Seismic evidence for a complex slide near the wreck of the Titanic: model of an instability corridor for non-channeled gravity events. *Mar Geol* 91:281-298

Shanmugam G (1997) The Bouma sequence and the turbidite mind set. *Earth Sci Rev* 42:201-229

Shanmugam G (2000) 50 years of the turbidite paradigm (1950s-1990s): deep-water process and facies models - a critical perspective. *Mar Petrol Geol* 17:285-342

Shepard FP (1975) Progress of internal waves along submarine canyons. *Mar Geol* 198:131-138

Shepard FP (1981) Submarine canyons: multiple causes and long-time persistence. *Am Assoc Petrol Geol Bull* 65(3):1062-1077

Shepard FP, Dill RF (1966) *Submarine canyons and other sea-valleys*. Rand McNally, Chicago

Shepard FP, McLoughlin PA, Marshall NF, Sullivan GG (1977) Current-meter recordings of low-speed turbidity currents. *Geology* 5:297-301

Shepard FP, Marshall N, McLoughlin PA, Sullivan GG (1979) Currents in submarine canyons and other sea valleys. *Am Assoc Petrol Geol Studies in Geology* 8

Stow DAV, Shanmugam G (1980) Sequence of structures in fine-grained turbidites. Comparison of recent deep-sea and ancient flysch sediments. *Sediment Geol* 25:23-42

Vassal J-P (1980) Les houles exceptionnelles et leurs conséquences. Estimation des conditions maximales de l'état de la mer dans le Golfe de Gascogne. Analyse d'une forte tempête récente: 30 novembre - 5 décembre 1976. Thèse Doct Université Bordeaux 1

Viana AR (1998) Le rôle et l'enregistrement des courants océaniques dans les dépôts de marges continentales: la marge du bassin sud-est brésilien. PhD thesis, Bordeaux University, No 1873, pp 354

Wiseman WJ Jr, Fan Y-B, Bornhold BD, Keller GH, Su Z-Q, Prior DB, Yu Z-X, Wright LD, Wang F-Q, Quian Q-Y (1986) Suspended sediment advection by tidal currents off the Huanghe (Yellow River) delta. *Geo-Mar Lett* 6:107-113

Wright LD, Yang Z-S, Bornhold BD, Keller GH, Prior DB, Wisenam WJ Jr (1986) Hyperpycnal plumes and plume fronts over the Huanghe (Yellow River) delta front. *Geo-Mar Lett* 6:97-105